International Journal of Biological Macromolecules 278 (2024) 134908

Contents lists available at ScienceDirect

International Journal of Biological Macromolecules

journal homepage: www.elsevier.com/locate/ijbiomac

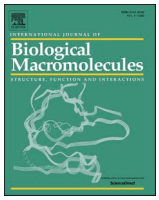

A thermosensitive chitosan hydrogel: An attempt for the nasal delivery of dimethyl fumarate

Noelia Nieto González [a], Giovanna Rassu [b,*], Massimo Cossu [b], Laura Catenacci [c], Milena L. Sorrenti [c], Eleonora Sofia Cama [c], Carla Serri [b], Paolo Giunchedi [b], Elisabetta Gavini [b]

[a] PhD Program in Chemical Science and Technology, Department of Chemical, Physical, Mathematical and Natural Sciences, University of Sassari, via Vienna 2, 07100 Sassari, Italy
[b] Department of Medicine, Surgery and Pharmacy, University of Sassari, via Muroni 23a, 07100 Sassari, Italy
[c] Department of Drug Sciences, University of Pavia, Via Taramelli 12, 27100 Pavia, Italy

ARTICLE INFO

Keywords:
Dimethyl fumarate
Thermosensitive hydrogel
Chitosan
Hydroxypropyl-β-cyclodextrin
Nasal delivery
Multiple sclerosis

ABSTRACT

Dimethyl fumarate (DMF) is a drug that is orally administered for the treatment of relapsing-remitting multiple sclerosis. However, DMF causes gastrointestinal side effects and flushing in 43 % of patients, which significantly contributes to treatment discontinuation. To reduce side effects and increase patient compliance, the aim of this study was to develop a thermosensitive chitosan/glycerophosphate hydrogel for the nasal administration of DMF. A binary system of DMF with hydroxypropyl-β-cyclodextrin (HP-β-CD) was made and included in the hydrogel precursor solution. The precursor solution (drug content, DMF stability, thermogelling properties, viscosity), and the resulting thermosensitive hydrogel (mucoadhesion, in vitro DMF permeation) were characterized. HP-β-CD was able to interact with DMF and improve its water solubility. The leader thermosensitive nasal solution, G1 solution, was loaded with approximately 92 % DMF, which remained stable for 21 days. The G1 solution formed a hydrogel in approximately 2–1 min; it had a pH of 6.8 ± 0.06 and caused no significant change in the osmolality of the simulated nasal medium. The G1 hydrogel showed good mucoadhesive properties and released DMF that permeated in vitro in a controlled manner. As a result, G1 is a potential new approach to exploit the intranasal administration of DMF for treating multiple sclerosis.

1. Introduction

Multiple sclerosis (MS) is a chronic autoimmune inflammatory demyelinating disease of the central nervous system (CNS) and one of the most common nontraumatic disabling diseases affecting mainly young adults [1]. Approximately 2.8 million people worldwide are affected by MS, 1,200,000 in Europe and approximately 130,000 in Italy [2]. According to various studies, the average age of onset of MS is between 28 and 31 years, and more women than men are affected [1,3]. The main pathogenic processes causing clinical symptoms include inflammation, demyelination and axonal degeneration [4,5]. There are currently no FDA-approved treatments for MS that are curative. Disease-modifying therapies available as oral treatments include fumaric acid esters such as dimethyl fumarate (DMF), the active metabolite of which is monomethyl fumarate (MMF) [6]. DMF hard gelatin capsules (Tecfidera®) have demonstrated efficacy in treating relapsing-remitting MS in adults [7]. Preclinical studies suggest that the combination of neuroprotective and immunomodulatory mechanisms is involved in the mode of action of DMF through activation of the nuclear factor (erythroid-derived 2)-like 2 (Nrf2) antioxidant pathway in the CNS [7,8]. Clinical trials have shown that DMF significantly reduces relapse rates and the development of new brain lesions on magnetic resonance imaging, leading to a reduction in the rate of disability progression [9]. In addition, several studies have shown that children and adolescents with MS may benefit from DMF treatment [10,11]. However, gastrointestinal side effects and flushing have been frequently reported, leading to poor compliance and discontinuation of therapy [9,12]. Therefore, this study aimed to investigate a formulation for the nasal administration of DMF to reduce side effects and increase patient compliance, taking into account the physicochemical properties of this drug (sublimation, chemical instability) [13]. In particular, for the first time, a thermosensitive chitosan/glycerophosphate hydrogel containing DMF complexed with hydroxypropyl-β-cyclodextrin (HP-β-CD) was developed to increase the bioavailability of the drug in the brain.

Nasal administration is an excellent alternative route for the

* Corresponding author.
E-mail address: grassu@uniss.it (G. Rassu).

https://doi.org/10.1016/j.ijbiomac.2024.134908
Received 20 May 2024; Received in revised form 26 July 2024; Accepted 18 August 2024
Available online 23 August 2024

Abbreviations

CH	chitosan
DMF	dimethyl fumarate
DMF + HP-β-CD 1:1	a binary system based on dimethyl fumarate and hydroxypropyl-β-cyclodextrin at a 1:1 molar ratio
DMF + HP-β-CD 1:2	the binary system based on dimethyl fumarate and hydroxypropyl-β-cyclodextrin at a 1:2 molar ratio
DSC	Differential Scanning Calorimetry
FTIR	Fourier Transform Infrared spectroscopy
G1 S	the thermosensitive hydrogel precursor solution prepared by dissolving DMF + HP-β-CD 1:1 in Milli-Q water
G1	the DMF-loaded leader thermosensitive nasal hydrogel
G1b S	the unloaded thermosensitive hydrogel precursor solution prepared by dissolving HP-β-CD in Milli-Q water
G1b	the unloaded leader thermosensitive nasal hydrogel
G2 S	the thermosensitive hydrogel precursor solution prepared by dissolving DMF + HP-β-CD 1:1 in 0.1 N HCl
G2b S	the unloaded thermosensitive hydrogel precursor solution prepared by dissolving HP-β-CD in 0.1 N HCl
GP	glycerophosphate hydrated disodic salt
HCl	hydrochloric acid
HP-β-CD	hydroxypropyl-β-cyclodextrin
TGA	thermal gravimetric analysis

treatment of both neurological and chronic diseases. It is a patient-friendly strategy due to the rapid beginning of the drug effect, painless nature, noninvasiveness, and simplicity of administration (self-medication) [14,15]. Among nasal formulations, stimuli-responsive in situ nasal gels increase drug retention, reduce mucociliary clearance and increase drug bioavailability in the brain [14]. The in situ gel is liquid upon administration but undergoes a sol-gel transition upon contact with the body. The sol-gel transition occurs due to an external stimulus, such as a change in temperature [16].

DMF was complexed with HP-β-CD, a highly soluble β-cyclodextrin derivative, to increase its water solubility. As a penetration enhancer, HP-β-CD is also helpful for improving the passage of DMF across biological membranes and, consequently, its in vivo bioavailability. HP-β-CD also shows potential therapeutic use in neurodegenerative diseases [17–20].

Chitosan (CH) is an amino polysaccharide with excellent mucoadhesive properties due to the interaction between its positive and negative mucin charge. This cationic polymer can act as a penetration enhancer, opening tight junctions between mucosal cells and promoting drug absorption. Consequently, CH is an optimal candidate for nasal drug delivery given its high biocompatibility, non-toxicity, and mucoadhesive and penetration-enhancing properties [21–27]. CH is a good candidate for in situ gel formation due to its capacity to form polyelectrolyte complexes with polyol salts such as glycerophosphate (GP) [14,16]. GP allows us to obtain a liquid solution at room temperature with a pH range of 6.8 to 7 and exhibits mild alkalinity (pK_a 6.34); it permits proper buffering without causing CH precipitation or gelation at low temperatures (between 4 and 15 °C) and promotes the protective hydration of CH chains [16]. The increase in temperature causes the rearrangement of the CH chains; this results in an increase in polymer-polymer interactions compared to solvent-polymer interactions, which in turn causes gel formation [14,16,28].

In this study, the optimized DMF and HP-β-CD binary system was selected and included in a thermosensitive hydrogel precursor solution based on chitosan and glycerophosphate. The thermosensitive nasal precursor solution was selected as the optimal formulation after the preformulative studies. The attributes of the precursor solution were investigated, including the drug content, chemical stability of DMF, thermogelling properties, pH, osmolality, and viscosity. Furthermore, the water uptake and mucoadhesive capabilities of the formed thermosensitive hydrogel were evaluated, as well as in vitro DMF permeation through a synthetic membrane simulating the nasal mucosa, to verify its suitability as a nasal delivery system.

2. Materials and methods

2.1. Materials

Dimethyl fumarate (DMF, 97 %), glycerophosphate hydrated disodic salt (GP), and mucin from porcine type II were purchased from Sigma–Aldrich (St. Louis, MO, USA). Hydroxypropyl-β-cyclodextrin (HP-β-CD, Cavasol® W7 HP Pharma, Mw: 1400 g/mol) was purchased from Wacker-Chemie GmbH (Munich, Germany). Chitosan (CH, ChitoClear® TM 1358, Mw: 103 kDa, deacetylation degree, 94 %) was obtained from PRIMEX EHF (Siglufjordur, Iceland). Hydrochloric acid (HCl) (37 %) was purchased from Honeywell Fluka™ (Seelze, Germany). Ultrapure water was obtained from a Milli-Q R4 system (Millipore, Milan, Italy). Chromatographic grade acetonitrile, ethanol and methanol were acquired from Merck (Darmstadt, Germany).

2.2. Study of the DMF and HP-β-CD binary system

2.2.1. Preparation of binary systems

Physical mixtures of DMF and HP-β-CD were prepared in a Turbula; the amounts of DMF and HP-β-CD were mixed in an equimolar ratio (DMF + HP-β-CD 1:1 (mol/mol)) or using an excess amount of HP-β-CD for the DMF + HP-β-CD 1:2 (mol/mol) binary system. To prepare DMF inclusion complexes with HP-β-CD, a semisolid technique, such as the kneading method, was employed. Approximately 20 mg of DMF and the corresponding amount of HP-β-CD (corresponding to 1:1 and 1:2 (mol/mol)) were wetted with ethanol to obtain a doughy mass, which was then dried at room temperature until reaching a constant weight. This process was repeated three times, and the resulting samples were sieved through a 250-μm sieve.

2.2.2. Physicochemical characterization of binary systems

To assess the thermal properties of the DMF + HP-β-CD binary systems, differential scanning calorimetry (DSC) analyses were performed with a Mettler STAR^e system (Mettler Toledo, Milan, Italy) equipped with a DSC821^e Module and an intracooler device for subambient temperature analysis (Julabo FT 900, Seelbach, Germany). Samples ranging from 2 to 4 mg were placed in sealed Al pans with pierced lids. The analyses were performed at least in triplicate in the temperature range of 30–350 °C (heating rate β = 10 K/min) under a nitrogen atmosphere (N_2 flow rate of 50 mL/min).

A Mettler STAR^e TGA system with simultaneous DSC (TGA/DSC1) (Mettler Toledo, Milan, Italy) was used to measure the mass losses. The measurements were performed at least in triplicate on 3–4 mg samples placed in alumina crucibles with pierced lids using the same experimental conditions for DSC analyses.

All the instruments were previously calibrated with indium as a standard reference.

Fourier transform infrared (FTIR) spectroscopy was performed using a Spectrum One spectrophotometer in the spectral range of 650–4000 cm^{-1} (64 scans with a resolution of 4 cm^{-1}) (Perkin Elmer, Monza, Italy) equipped with a MIRacle™ ATR device (Pike Technologies, Madison, Wisconsin, USA). The spectra were acquired in triplicate in transmittance mode by pressing the samples on an ATR crystal of ZnSe.

2.2.3. Phase solubility analysis

Phase solubility studies were conducted by the method described by

Higuchi and Connors [29]. DMF (0.050 g) was added to a vial containing Milli-Q water and various concentrations of HP-β-CD (with molar ratios of DMF + HP-β-CD of 1:0.5, 1:1, and 1:2). The vial was agitated in a rotary shaker for 72 h at 25 °C until equilibrium was reached; centrifugation was performed at 4400 rpm for 10 min at 20 °C (Eppendorf Centrifuge 5702 R, Hamburg, Germany). The supernatants were also centrifuged at 14,000 rpm for 10 min in a microcentrifuge (Hettich Mikro 120 centrifuge, Tuttlingen, Germany).

The quantity of DMF in the solution was quantified using high-performance liquid chromatography (HPLC), as detailed below.

2.3. Preparation of hydrogel precursor solutions

A thermosensitive nasal hydrogel based on CH and GP was prepared from a previously developed thermosensitive hydrogel. The hydrogel was thoroughly characterized in terms of its thermogelling properties, rheological behavior, and biodegradability [16]. The CH/GP weight ratio was chosen based on preformulation studies detailed in the Supporting Information. Two precursor solutions, G1 S and G2 S, were prepared with CH and GP at the optimized weight ratio, containing DMF (Table 1). G1 S and G2 S differed in the method used to acidify the aqueous solution necessary for the solubilization of chitosan, as described below and illustrated in Fig. 1.

For the preparation of G1 S, DMF (0.021 g) and HP-β-CD (0.205 g), in a 1:1 molar ratio, were mixed in a mortar. The obtained binary system was then dissolved in 10 mL of Milli-Q water in a 15 mL polypropylene centrifuge tube with a stopper to prevent DMF sublimation [13]. The tube was kept stirring in a rotary shaker at room temperature until the DMF was completely dissolved (reached in 48 h). The aqueous solution was then acidified with 100 μL of 0.1 N HCl immediately before adding CH (0.2 g) under magnetic stirring. Instead, for preparing G2 S, DMF (0.021 g) and HP-β-CD (0.205 g), in a 1:1 molar ratio, were mixed in a mortar. This binary system was then dissolved in 10 mL of 0.1 N HCl again in a 15 mL polypropylene centrifuge tube with a stopper. The tube was kept stirring in a rotary shaker at room temperature for 24 h; subsequently, CH (0.2 g) was added under magnetic stirring.

For both G1 S and G2 S, the obtained solutions were cooled in an ice bath until they reached 4 °C. Then, 1 mL of GP solution (10 % *w/v* in Milli-Q water) was slowly added dropwise with vigorous magnetic stirring for 15 min at 4 °C. The resulting precursor solutions were stored at 4 °C to avoid gelation [16].

The identical precursor solutions were also prepared without DMF and named G1b S and G2b S.

2.4. HPLC analysis of DMF

DMF was quantified by a rapid and sensitive, high-performance liquid chromatography (HPLC)-modified method [30]. A Varian HPLC–DAD system (Palo Alto, CA, USA) comprising two ProStar 210 pumps, a ProStar 410 autosampler and a DAD Varian 330 detector was used. The data were acquired and processed using Varian Workstation version 6.2 software. Chromatographic separation was performed using a Hypersil C18 column (150 × 4.6 mm, 5 μm particle size, Thermo Fisher Scientific, Milan, Italy) preceded by a guard column (20 × 4.0 mm, 5 μm). The mobile phase, a binary solution of acetonitrile and water at a volume ratio of 50:50 *v*/v, was filtered through 0.22 μm cellulose regenerated membrane filters (Sartorius, Goettingen, Germany) before use. The flow rate was 1.5 mL/min at room temperature, and the detection wavelength was 210 nm. The injection volume was 10 μL, and the analysis time was 4 min per sample. The assay exhibited linearity within the concentration range of 2.5–50 mg/L (DMF: $y = 309{,}866.30x - 449{,}787$; $R^2 = 0.9993$).

Table 1
Composition of the hydrogel precursor solutions. The drug content results are expressed as the mean ± SD ($n = 6$).

Formulation	DMF-HP-β-CD ratio	CH/GP ratio (*w/v*) (%)	Medium	DC	
				mg/mL	%
G1 S	1:1	2/10	Milli-Q water	1.77 ± 0.10	92.52 ± 5.21*
G2 S	1:1	2/10	HCl 0.1 N	0.71 ± 0.28	36.52 ± 13.84*

* p value <0.05: drug content (%) G1 vs G2.

2.5. Drug content

The DMF content of G1 S and G2 S was determined by HPLC analysis. A 100 μL volume of the solution was diluted in 10 mL of acetonitrile in a volumetric flask. The resulting mixture was sonicated for 30 min in an ultrasonic bath and then centrifuged at 14,000 rpm for 10 min in a microcentrifuge (Hettich Mikro 120 centrifuge, Tuttlingen, Germany) for the first extraction. Next, the supernatant was analyzed by HPLC. Additionally, a second extraction was conducted. The resulting supernatant was analyzed to quantify any residual DMF present. The drug content (DC) was calculated as the amount of DMF per mL of solution and as a percentage with respect to the DMF used for the preparation.

2.6. Characterization of the hydrogel precursor solution

Based on the drug content results, G1 S was chosen as the leader hydrogel precursor solution, and it was characterized to assess whether it was suitable for nasal administration.

2.6.1. Chemical stability of DMF

The chemical stability of DMF in G1 S stored at 4 °C was evaluated; aqueous solutions of free DMF and DMF + HP-β-CD 1:1 were stored at 4 °C and analyzed for comparison. At predetermined time intervals (1, 3, 7, 14, 21 and 28 days), 100 μL of G1 S was collected and diluted in 10 mL of acetonitrile in a volumetric flask; the sample was then processed as described in Section 2.5. The amount of DMF was quantified using the HPLC method described above.

2.6.2. Gelation time

The gelation time of both G1b S and G1 S was investigated using the inverted tube test method [16]. Chromatographic glass tubes (2 mL) were heated in a temperature-controlled bath at 35 °C. Samples of G1b S and G1 S (500 μL) were added to the tubes, which were then placed in a bath for incubation. At predetermined intervals of 30 s, the tubes were removed from the water bath and horizontally inverted to observe the flowability of the solutions. If the solution did not flow within 15 s, the time was recorded as the gelation time. The test was also repeated over 28 days to assess the stability of the solutions and to monitor any changes in gelation time over time.

2.6.3. pH and osmolality measurements

The pH values of G1 S and G1b S were measured to verify whether they were appropriate for nasal administration. The pH was measured at 4 °C with a calibrated pH meter (Hanna Instruments, HI 8417, Singapore).

The osmolality of the simulated nasal mucus was measured before and after contact with G1 S and G1b S [31]. Simulated nasal mucus was prepared by dissolving 8 % (*w*/w) porcine mucin-type II in a simulated nasal electrolyte solution with 7.5 mg/mL sodium chloride, 1.3 mg/mL potassium chloride, and 0.3 mg/mL calcium chloride dihydrate [32]. A NaOH solution (0.1 M) was used to adjust the pH to approximately 6.4 [32]. G1b S and G1 S (1 mL) were soaked in simulated nasal mucus (9 mL) in a 15 mL polypropylene centrifuge tube and incubated for 24 h at 37 °C. Then, the simulated nasal mucus (50 μL) was analyzed with an osmometer (OSMOMAT 030 Cryoscopic Osmometer, Genotec, Germany).

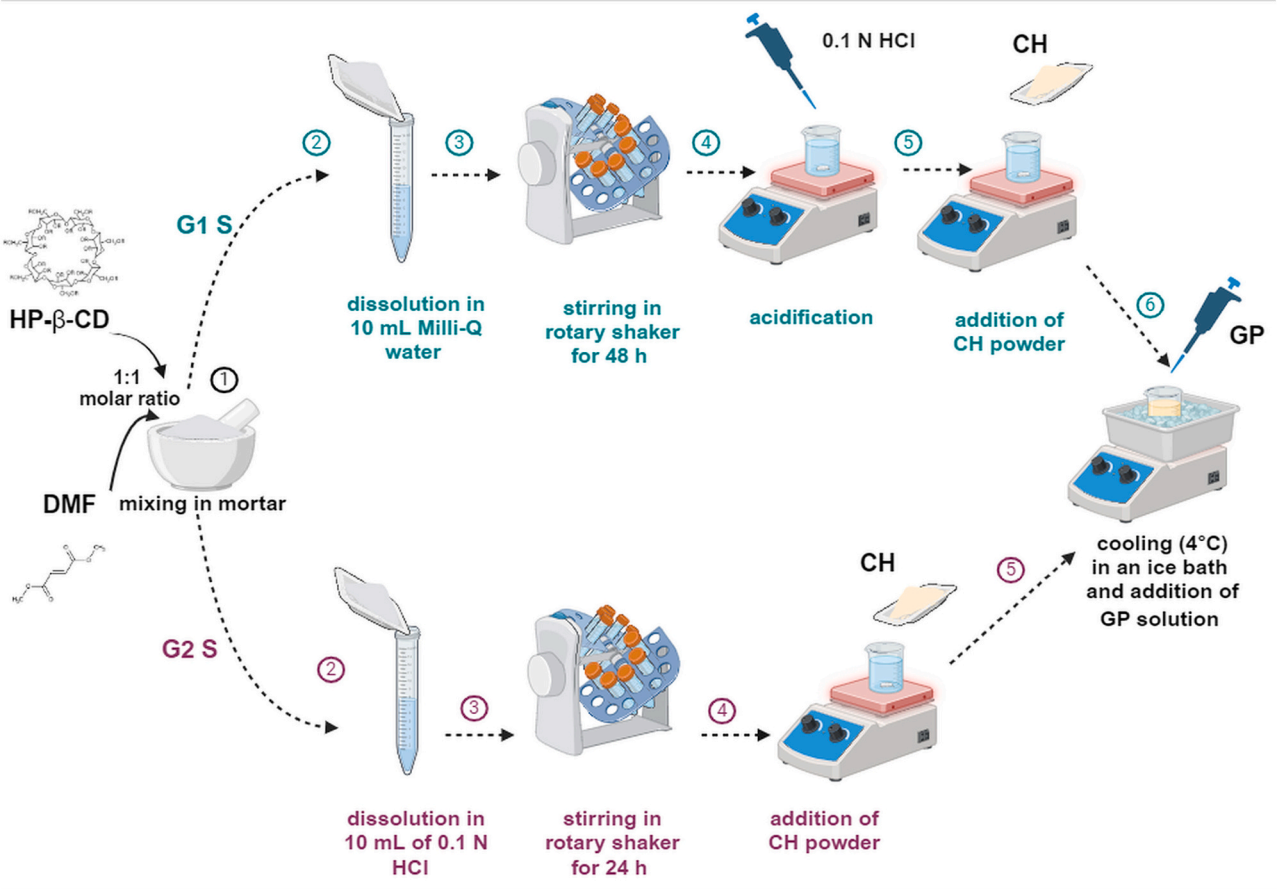

Fig. 1. Preparation of hydrogel precursor solutions. Created with BioRender.com

2.6.4. Viscosity measurements

The solution viscosity of G1 S over time (0, 1, 3, 7, 14, and 28 days, kept at 4 °C) was determined to assess the solution stability. A rotational viscosimeter Fungilab (Barcelona, Spain) was used with L1–2 spindles at 100 rpm. Likewise, the solution viscosity of G1b S was determined for comparison. The test was conducted in triplicate by keeping the solutions at a temperature of 4 °C in an ice bath to avoid viscosity changes due to the temperature difference between the refrigerator and the working environment.

2.7. Characterization of the thermosensitive nasal hydrogel

2.7.1. Physicochemical characterization

Physicochemical characterization of G1 and G1b was carried out using the same techniques described in Section 2.2.2.

2.7.2. Water uptake determination

The capacity of G1 to absorb water was determined using a modified Enslin apparatus [25]. A modified Enslin apparatus consists of a fritted glass support connected to a 0.1 mL glass graduated capillary via a three-way channel. The apparatus was filled with ultrapure water maintained at a constant temperature of 34 °C. The upper surface of the fritted glass support was aligned horizontally with the capillary to facilitate free movement of water. A cellulose filter ($d = 1$ cm) was pre-saturated with water at 34 °C and placed on the glass support. A volume of G1 S (approximately 30 μL) was uniformly spread on the pre-saturated cellulose filter. The glass support was covered with parafilm to prevent evaporation during the experiment. The amount of water absorbed by the formed hydrogel was recorded at fixed time intervals (ranging from 2.5 to 180 min).

2.7.3. Mucoadhesion studies

The mucoadhesion test was performed using a modified precision balance [33]. G1 S (30 μL) was applied to the surface of the probe (diameter = 1.5 cm) and kept at 34 °C for 60 s to allow gelation; a filter paper conditioned with 2 % mucin solution or with pH 6.5 phosphate buffer (control) was fixed on the base of the balance. After a contact force of 65 mN/cm^2 for 60 s, the detachment force (in mN/cm^2) between the hydrogel and the filter was measured.

2.7.4. Spray droplet size

G1 S was placed in an amber glass bottle with a nasal plastic dispenser (Farmalabor, Canosa di Puglia, Italy) and sprayed in a flask heated at 35 °C (see video); the resulting hydrogel particles were dispersed in Milli-Q water and analyzed by a Coulter LS 100Q laser sizer (Beckman Coulter Particle Characterization, Miami, FL) for the measurement of particle size and size distribution. The size is expressed as the equivalent volume/surface diameter (D_{vs}) in μm, and the droplet size distribution is described as Dv_{10}, Dv_{50}, Dv_{90} and the SPAN factor [34], as recommended by the FDA for nasal sprays [35]. The results are the means of triplicate experiments performed three times ($n = 9$) ± SD.

2.7.5. In vitro permeation studies

In vitro permeation studies were performed using vertical diffusion cells (EP3909667A1, University of Sassari) with donor and acceptor compartments connected to a continuous flow system and with a permeation area of 1.5 cm^2 [26]. The test was performed on G1 S and an aqueous solution of DMF + HP-β-CD 1:1 for comparison. Cellulose acetate membranes with a 0.45 μm pore size (Sartorius, Goettingen, Germany), conditioned with pH 6.5 phosphate buffer, were placed between the two cell compartments. The receptor compartment was filled with

50 mL of pH 6.5 phosphate buffer and thermostated at 37 °C [26]; meanwhile, G1 S and DMF + HP-β-CD 1:1 aqueous solution (both containing 20 mg of DMF) were added to the donor compartment. Aliquots (600 μL) of the acceptor medium were withdrawn at 15, 30, 60, 90 and 120 min, and an equal amount of fresh acceptor fluid was added to ensure *sink* conditions. The amount of DMF in the acceptor medium was determined by HPLC.

Considering the permeation profile of DMF-HP-β-CD, the equation of the linear portion from 15 to 120 min was calculated. Thus, the release profiles were corrected to remove the degradation aspect of DMF in the acceptor medium. According to the literature, the technique used for the correction can be described by the equation below:

$$Ftn = Ft \times \frac{100}{-0.2514 \times t + 60.237}$$

where Ftn is the corrected percentage release, Ft is the cumulative percentage release, and t is the time at which the Ft level was taken [36]. The results are expressed as the percentage of DMF permeated versus time (mean ± SD).

2.8. Statistical analysis

The results represent of at least three measurements (mean ± standard deviation (SD)). Statistical analyses were performed using GraphPad Prism 8.0 software (GraphPad Software, Inc., San Diego, CA, USA). The nonparametric Kruskal–Wallis test was used to compares three groups; Dunn's multiple comparisons test was performed post-hoc to determine which group differed from each other. On the contrary, the nonparametric Mann–Whitney test was used to compare two groups. Nonparametric tests are more robust with small samples for which it is difficult to verify the assumption of normality. Confidence intervals of 95 % were selected. For all tests, a $P < 0.05$ was considered statistically significant.

3. Results

3.1. Study of the DMF and HP-β-CD binary system

3.1.1. Physicochemical characterization of binary systems

The thermal parameters of commercial DMF were used as references for the pure compounds in the study of the interaction products. Commercial DMF is a white crystalline powder with a thermal profile typical of an anhydrous compound, exhibiting an endothermic effect at 103.2 ± 0.7 °C due to melting (T_{onset} = 100.5 ± 0.5 °C; ΔH_{fus} = 208 ± 2 J/g) followed by sample decomposition at approximately 130 °C (Fig. 2A, curve a). HP-β-CD is an amorphous cyclodextrin characterized by a DSC profile (Fig. 2A, curve b) with a broad endotherm between 60 and 100 °C due to dehydration of the sample. The presence of the drug melting endotherm is evident in the PM (Fig. 2A, curve c), with a melting enthalpy decrease of approximately 37 % relative to that of pure DMF (ΔH_{fus} = 131 ± 1 J/g), probably due to a partial interaction between HP-β-CD and DMF by simple physical mixing. The DSC curve of the product DMF + HP-β-CD 1:1 (mol/mol) obtained by kneading (Fig. 2A, curve d) still revealed an endothermic effect attributable to DMF melting but of a small entity (ΔH_{fus} = 26 ± 2 J/g), indicating an interaction between the two components in the system.

TGA (Fig. 3, curve a), recorded in the same temperature range as the DSC, confirmed the anhydrous nature of the drug by highlighting a single mass loss starting at approximately 84 °C due to decomposition immediately after sample melting. The TGA curve of HP-β-CD (Fig. 3, curve b) showed an initial mass loss of approximately 5 % between 40 and 90 °C due to dehydration, followed by a second much more significant mass loss starting from a temperature of approximately 264 °C, attributable to sample decomposition. According to the TGA curve of the equimolar PM (Fig. 3, curve c), there was an initial mass loss of approximately 13 % between 40 and 110 °C due to the concomitant loss of water and the drug, followed by a second largest mass loss from a temperature of approximately 290 °C due to the decomposition of the sample. The TGA curve of the product DMF-HP-β-CD 1:1 (mol/mol) obtained by kneading (Fig. 3, curve d) showed an initial mass loss of approximately 2 % in the temperature range of 40–60 °C, corresponding to the loss of the water contained in the cyclodextrin, followed by a loss of mass in the temperature range of 60–110 °C, mainly due to the loss of approximately 70 % of the drug. The remaining part of the drug present in the sample was almost completely retained by the cyclodextrin with which it interacts and then was lost starting at approximately 290 °C, concurrent with the decomposition of the sample.

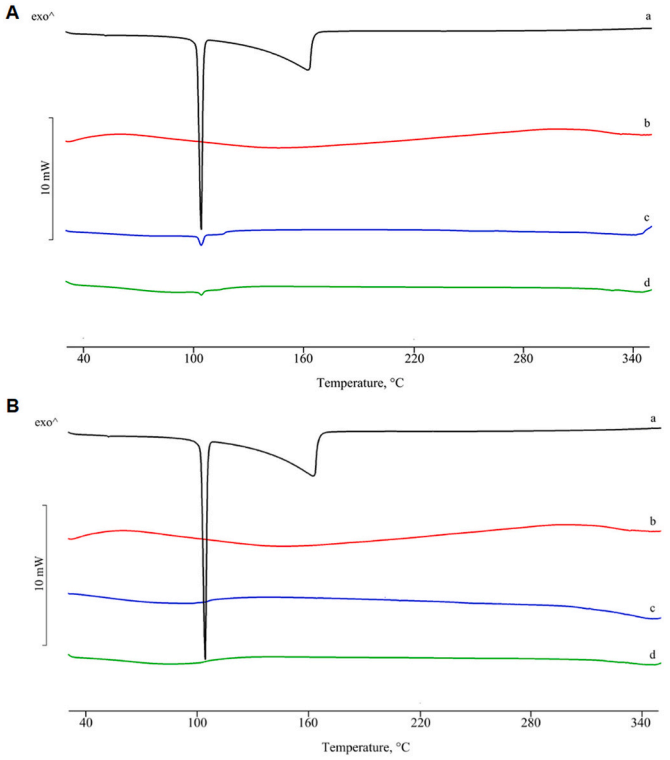

Fig. 2. DSC curves of DMF (curve a), HP-β-CD (curve b), their physical mixture (curve c) and the kneading product DMF + HP-β-CD 1:1 (mol/mol) (curve d) (A). DSC curves of DMF (curve a), HP-β-CD (curve b), their physical mixture (PM) (curve c) and the kneading product (KN) DMF + HP-β-CD 1:2 (mol/mol) (curve d) (B).

The partial interaction between DMF and HP-β-CD was confirmed by FTIR analysis of the same samples (Fig. 4A), for which it was possible to observe a shift of the characteristic absorption bands of DMF at 1713 and 1304 cm^{-1} toward slightly higher wavenumbers, namely, 1716 and 1310 cm^{-1}, respectively.

Fig. 2B shows the DSC curves recorded for the binary system DMF-HP-β-CD 1:2 (mol/mol). The drug fusion endotherm is only hinted at in the PM DSC curve (Fig. 2B, curve c) while it disappears in the product DMF-HP-β-CD 1:2 (mol/mol) obtained by kneading (Fig. 2B, curve d) because of a complete interaction with HP-β-CD in the molar ratio, resulting in an excess of CD.

The FTIR spectrum of the product DMF-HP-β-CD 1:2 (mol/mol) obtained by kneading (Fig. 4B) showed that the characteristic bands of DMF shifted to higher wavenumbers, indicating an interaction between the two components. In particular, the band at 1713 cm^{-1} due to the stretching vibrations of carbonyl C═O shifted to 1725 cm^{-1}, the band at 1304 cm^{-1} due to the stretching vibrations of the C—O ester shifted to 1309 cm^{-1}, and the band at 773 cm^{-1} due to C═O bending shifted to 776 cm^{-1}.

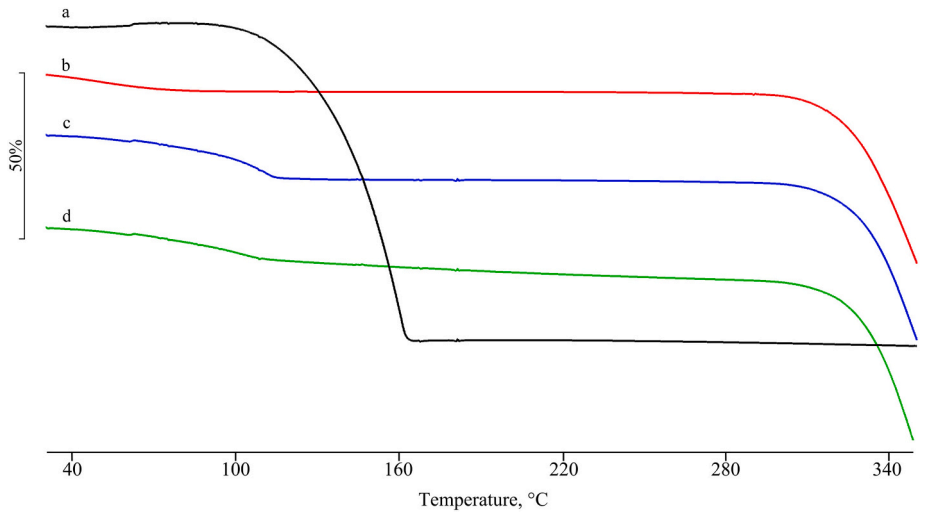

Fig. 3. TGA curves of DMF (curve a), HP-β-CD (curve b), their physical mixture (curve c) and the kneading product DMF + HP-β-CD 1:1 (mol/mol) (curve d).

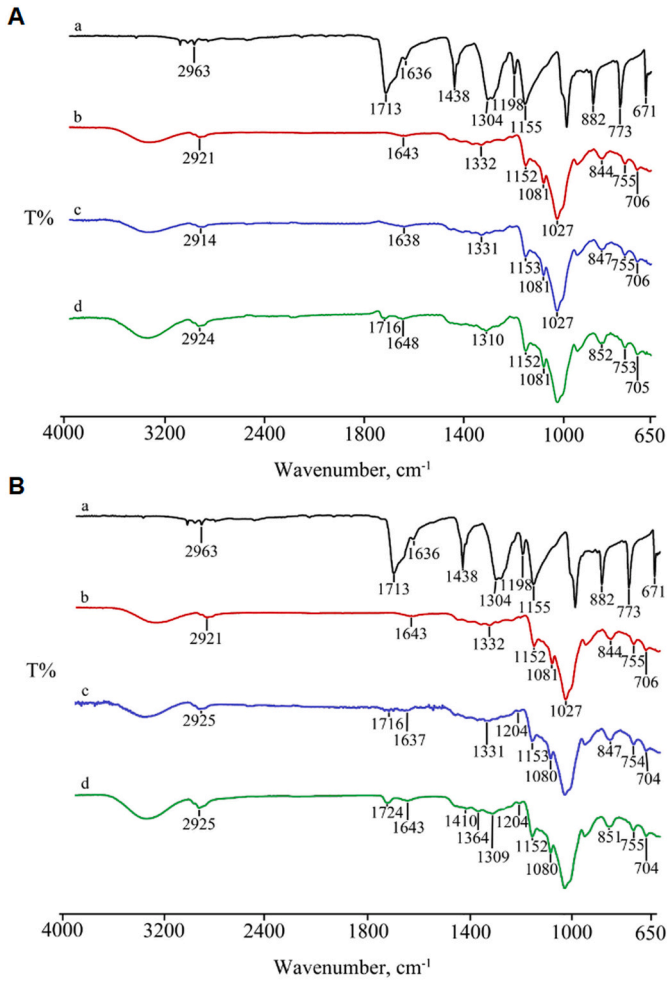

Fig. 4. FTIR spectra of DMF (spectrum a), HP-β-CD (spectrum b), their physical mixture (PM) (spectrum c) and their kneading product (KN) DMF + HP-β-CD 1:1 (mol/mol) (spectrum d) (A). FTIR spectra of DMF (spectrum a), HP-β-CD (spectrum b), their physical mixture (PM) (spectrum c) and their kneading product (KN) DMF + HP-β-CD 1:2 (mol/mol) (spectrum d) (B).

3.1.2. Phase solubility analysis

Phase solubility studies were carried out using the method developed by Higuchi [29]. The presence of HP-β-CD improved the water solubility of DMF from 1.58 g/L [30] to 1.89 ± 0.01, 2.17 ± 0.10, and 2.94 ± 0.06 g/L when DMF-HP-β-CD molar ratios of 1:0.5, 1:1 and 1:2 were used, respectively.

Although the 1:2 molar ratio showed the best performance, the 1:1 molar ratio of DMF-HP-β-CD was selected to prepare thermosensitive nasal solutions to avoid interfering with hydrogel formation.

3.2. Drug content of hydrogel precursor solutions

The drug content of G1 S and G2 S was determined. As reported in Table 1, G1 S had a greater drug content than G2 S because of the preparation method employed ($P < 0.05$). Indeed, in the case of the G1 S preparation, DMF + HP-β-CD 1:1 was solubilized in an aqueous medium for 48 h, while during the preparation of G2 S, DMF + HP-β-CD 1:1 was solubilized in 0.1 N HCl for 24 h until complete solubilization. On the other hand, G1 S showed a drug content close to the theoretical value and was subsequently chosen for further characterization.

3.3. Characterization of the hydrogel precursor solution

3.3.1. Chemical stability of DMF

The chemical stability of DMF in G1 S stored at 4 °C was determined over a period of 28 days and compared with that of free DMF and DMF + HP-β-CD (1:1) aqueous solutions. The percentage of DMF in G1 S was stable for 21 days ($P > 0.05$) (from 92.52 ± 5.21 at t_0 to 86.18 ± 7.98 % at 21 days concerning the amount of DMF dissolved Milli-Q for the preparation of G1 S); after that, a significant reduction in the DMF content was observed (72.82 ± 10.14 % at 28 days; $P < 0.05$ t_0 vs 28 days). In contrast, free DMF and DMF + HP-β-CD at a ratio of 1:1 were stable, as >90 % of the DMF was present after 28 days ($P > 0.05$).

3.3.2. Gelation time

The gelation time for G1 S and G1b S was evaluated for 28 days (Table 2). Hydrogel formation by G1 S took approximately 2 min (Fig. 5)

Table 2
The gelation times (in min) of G1 S and G1b S were measured with an inverted tube test over time.

Days	0	3	7	14	21	28
G1b S	1:00	1:00	1:00	1:00	1:00	1:00
G1 S	2:00	1:30	1:00	1:00	1:00	1:00

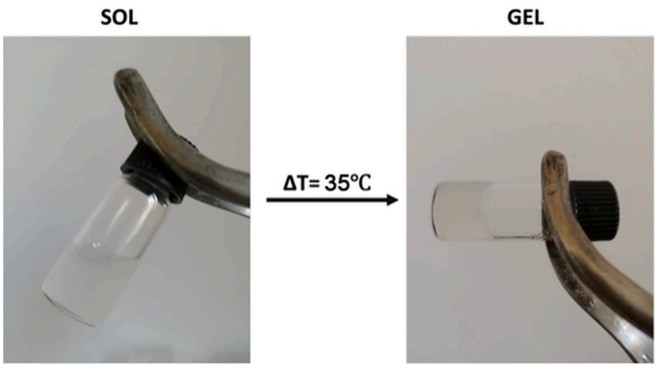

Fig. 5. Photographs of the gelation process of G1 S during the inverted tube test.

but decreased at 1 min over time, remaining temperature-sensitive after 4 weeks of storage at 4 °C. In addition, G1b S exhibited a gelation time of 1 min over time.

3.3.3. pH and osmolality measurements

The pH values of G1b S and G1 S were 6.9 ± 0.05 and 6.8 ± 0.06, respectively; therefore, DMF loading did not affect the solution pH ($P > 0.05$).

The osmolality changes in the simulated nasal medium were measured using the extraction method. The simulated nasal mucus had an osmolality of 0.447 ± 0.002 Osm/kg, whereas the osmolalities of the simulated nasal media with G1b S and G1 S were 0.613 ± 0.05 and 0.585 ± 0.016 Osm/kg, respectively. The results showed that the hydrogels did not significantly modify the osmolality of the simulated nasal media ($P > 0.05$), which remained in the range of 300–700 mOsmol/kg [37].

3.3.4. Viscosity measurements

The viscosity of G1 S was 65.84 ± 8.82 cP and did not vary significantly over time (59.45 ± 2.41 at 28 days; $P > 0.05$). In contrast, G1b S at t_0 showed greater viscosity than G1 S (206.00 ± 8.73 cP; $P < 0.05$); the viscosity gradually decreased over time, reaching the same value as G1 S after 21 days (68.72 ± 3.28 cP), probably due to a reorganization of the components of the structures.

3.4. Characterization of the thermosensitive nasal hydrogel

3.4.1. Physicochemical characterization

Fig. 6a shows the DSC curves recorded for G1 (curve b) and G1b (curve a) in comparison with the same hydrogel formulation mixed with the drug (G1b + DMF, curve c). Only for this last sample did a very low endothermic effect appear at a temperature corresponding to drug melting (curve c); in G1, only a very large endothermic effect was recorded due to sample decomposition between 140 and 160 °C, confirming the homogeneous dispersion of DMF in the hydrogel network.

TGA curves agree with DSC thermal profiles (Fig. 6b), showing total mass loss of the samples in the same temperature range as the endothermic effect in DSC.

The FTIR spectra recorded for the same samples are shown in Fig. 6c. The same graph also shows a spectrum obtained by the instrument elaboration of the differences recorded between the two samples. In this spectrum, some bands appear due to the presence of DMF, which are instead obscured in G1, where the hydrogel matrix covers any other band. In this spectrum, some bands attributable to DMF can be observed, revealing the presence of the drug loaded in the hydrogel formulation.

3.4.2. Water uptake determination

The water uptake of G1 is presented in Fig. 7. In the first 15 min, G1 absorbed approximately 0.16 ± 0.11 μL/mg of water and then

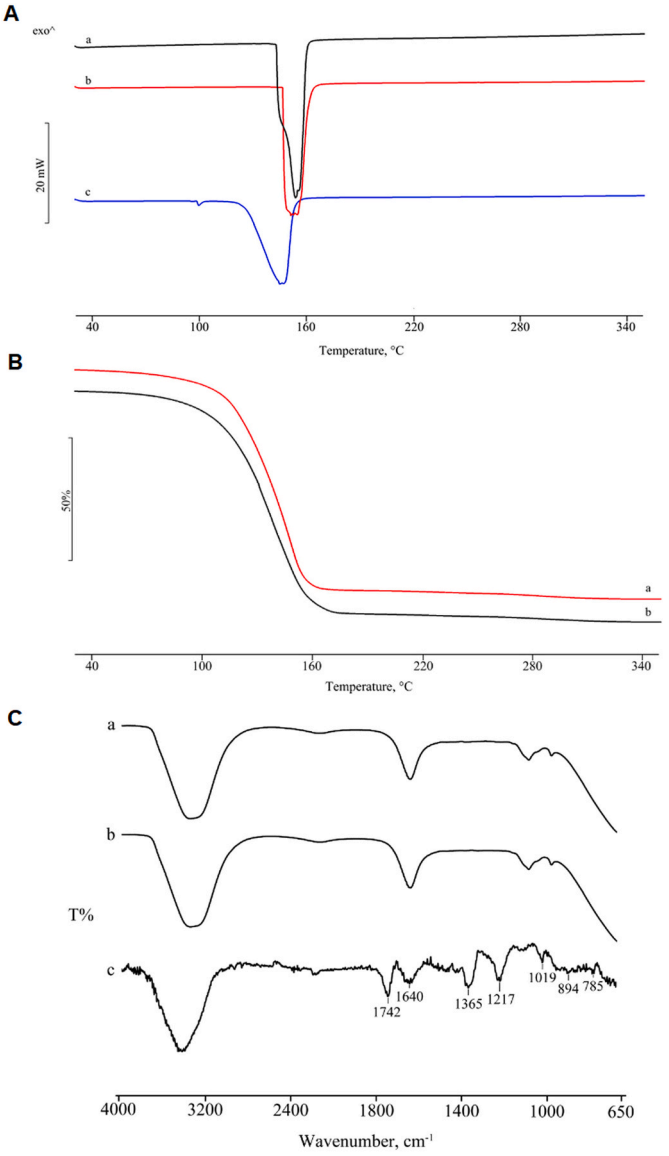

Fig. 6. DSC curves of G1b (curve a), G1 (curve b) and the physical mixture G1b + DMF (curve c) (A). TGA curves of G1b (curve a) and G1 (curve b) (B). FTIR spectra of G1b (spectrum a) and G1 (spectrum b) and the instrumental difference between the two spectra (spectrum c) (C).

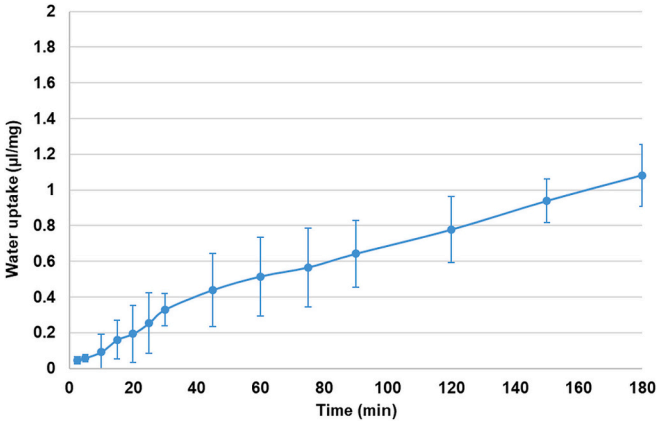

Fig. 7. The water uptake capacity (μL/mg) of G1. The results are reported as the mean value ± SD ($n = 3$).

continued to gradually absorb small amounts until 1.08 ± 0.17 μL/mg after 180 min ($R^2 = 0.976$ of trend line). G1 showed a low water uptake capacity due to water in the solution/hydrogel.

3.4.3. Mucoadhesion studies

The detachment force needed for the separation of G1 from filter paper saturated with mucin was 263.25 ± 2.51 mN/cm^2, which was significantly greater than that of the control (108.48 ± 4.34 mN/cm^2) ($P < 0.05$).

3.4.4. Spray droplet size

After being sprayed on a warm surface, the droplets of G1 S turned into hydrogel particles with a D_{vs} of 66.65 ± 3.28 μm. Ten per cent of the distribution had a volume median diameter lower than 36.31 ± 6.25 μm (Dv_{10}) and 50 % lower than 123.80 ± 23.74 μm (Dv_{50}); Dv_{90} was 274.50 ± 80.35 μm. Only 1.14 % of the particles had a diameter lower than 10 μm; thus, the possibility that the particles may be inhaled into the lung is very limited. The SPAN index was 1.90 ± 0.33, indicating a narrow size distribution [34].

3.4.5. In vitro permeation studies

In vitro permeation studies of DMF released from G1 and DMF + HP-β-CD 1:1 aqueous solution were performed, and the results are reported in Fig. 8 (dotted lines). After 15 min, the percentages of DMF permeated from the G1 and DMF + HP-β-CD 1:1 were 16.77 ± 2.31 % and 55.41 ± 6.08 %, respectively; then, the percentage of DMF from G1 reached 37.28 ± 9.11 % after 120 min, while the percentage of DMF permeated from DMF-HP-β-CD decreased to 29.03 ± 9.58 %. This decrease was related to DMF degradation in the acceptor medium (pH 6.5, phosphate buffer) at 37 °C, so the permeation profiles were corrected (Fig. 8, continuous lines). As expected, approximately 90 % of the DMF + HP-β-CD 1:1 solution permeated after 20 min, and approximately 30 % from G1 reached 100 % after 100 min. Thus, the amount of DMF released from G1 permeated the membrane linearly from 15 min to 120 min ($R^2 = 0.986$), demonstrating the ability of the G1 hydrogel to control DMF release compared to that of the DMF + HP-β-CD 1:1 solution ($P < 0.05$).

4. Discussion

An in situ thermosensitive hydrogel was chosen as the nasal formulation for the delivery of DMF to explore an alternative route of administration of this drug given the gastrointestinal adverse events related to its oral administration in tablets. Gastrointestinal adverse events are significant and frequent (43 % of patients) and determine

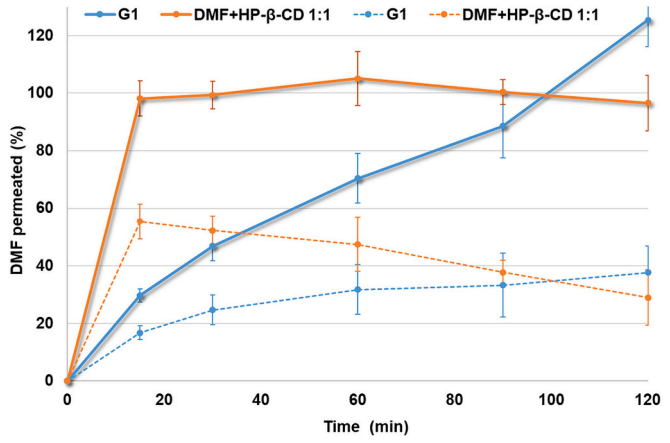

Fig. 8. In vitro permeation profile of DMF from G1 and DMF + HP-β-CD 1:1 aqueous solution (dotted lines) and data corrected (continuous lines). The results are the means of three experiments. The data are reported as the means ± SDs. * $P < 0.05$ G1 vs DMF + HP-β-CD 1:1 after 15 and 30 min.

discontinuation within the first 3 months of treatment, despite its efficacy in treating relapsing-remitting MS [9,12]. The physico-chemical properties of DMF, such as sublimation at room temperature (which limits the preparation of nasal powders) [38] and chemical instability [13], influence the choice and design of the formulation. The use of a thermosensitive hydrogel as a nasal drug delivery system was recently investigated, resulting in a versatile and convenient formulation [39]; it can be administered as a solution similar to traditional nasal sprays, but it is not quickly drained from the nasal cavity due to instantaneous gelation at nasal temperature [14,39–41]. The fast sol-gel transition of the hydrogel precursor solution reduces mucociliary clearance and increases the permanence time of the drug in contact with the nasal mucosa and, consequently, nasal drug bioavailability [14,39]. Furthermore, thermosensitive hydrogels promote the direct nose-to-brain transport of loaded drugs [14,40–42].

Thermosensitive CH/GP hydrogel precursor solutions were designed based on previously reported methods [16]. CH is a natural cationic polymer widely used as a nasal excipient due to its excellent biodegradability, biocompatibility, mucoadhesiveness and penetration enhancement [16,26,27,39]. In the presence of GP, CH forms a hydrogel that is liquid at low temperature but gel at physiological temperature; the gelation temperature and time are directly influenced by the concentration of GP [39,43,44]. Hydrogen bonding between CH chains, electrostatic attraction between CH ammonium and GP phosphate groups and CH-CH hydrophobic interactions may be involved in the gelation process [16,43].

Before the preparation of the hydrogel precursor solution, DMF was complexed with HP-β-CD to increase its water solubility necessary to obtain a high DMF concentration in the dose volume administered with a typical nasal dispenser (50–100 μL; maximum 200 μL) [45]. As demonstrated by DSC, TGA and FTIR, HP-β-CD partially interacted with DMF in the binary system at a ratio of 1:1 and completely when present in excess (1:2 molar ratio), but in each case, HP-β-CD increased the water solubility of DMF, which is consistent with the literature [19,46]. Although an excess of HP-β-CD increased the solubility, it interfered with hydrogel formation (data not reported), so a binary system with a 1:1 molar ratio was included in the hydrogel precursor solution. The preparation of the hydrogel precursor solution requires an acidic environment (pH < 6) for CH solubilization [16], but DMF is susceptible to hydrolysis under both acidic and alkaline conditions, with decreasing stability in the following pH order: 7 > 5 > 3 > 1 > 9 [47]. For this purpose, two preparation methods that differ only for the HCl addition step were compared. The results demonstrated that the acidic environment and prolonged availability of DMF in this environment decreased the drug content of G2 S; additionally, HP-β-CD could not to protect DMF from degradation. Cyclodextrins are capable of enhancing the stability of many drugs (e.g., β-lactam antibiotics and diloxanide furoate) in aqueous solutions, hampering different reactions such as hydrolysis [46]. The acidification shortly before the addition of CH and GP prevented degradation; in fact, the drug content of G1 S was close to the theoretical value and remained stable for 21 days. G1 S was, therefore, further characterized to verify the requirements of a nasal formulation (pH, osmolality, droplet size, viscosity, mucoadhesion and water uptake properties) and, specifically, of a thermosensitive nasal hydrogel (gelation time, drug release) [40,41,48].

pH and osmolality are fundamental requirements of nasal formulations for preventing nasal mucosa irritation and/or damage to cilia [48]. After the addition of GP to the hydrogel precursor solution, the pH of G1 S increased from 5 to 6.8; this prevented CH precipitation or gelation of G1 S at low temperatures (between 4 and 15 °C) and ensured biocompatibility with the nasal mucosa, whose pH was in the range of 5.5–6.5 [16,43,49–51]. Following gelation, GP quickly diffuses out of the hydrogel, increasing the osmolality of the nasal mucus and possibly causing toxicity to the mucosa [31,52]. The results demonstrated that G1 S did not affect the osmolality of the simulated nasal mucus, preventing nasal irritation and simultaneously enhancing DMF

permeability through the nasal mucosa [31,53].

G1 S exhibited an optimum viscosity to permit easy administration of the liquid using a typical nasal spray device; after gelation, this viscosity increased, enhancing the residence time of DMF in the nasal cavity by reducing mucociliary clearance [53]. In the literature, a favorable viscosity index and range for nasal formulation have not been reported; however, a low viscosity determines rapid drainage from the nasal cavity, whereas an excessive viscosity could affect the administration, drug release and discomfort [40]. After spray with the nasal dispenser, the size of the G1 droplets complied with the standard range of 10–200 μm for nasal liquid formulations, and the possibility that the particles may be inhaled into the lung is very limited [35]. G1 S gelled at the temperature of the nasal mucosa (32–35 °C), with a gelation time of 1–2 min if measured by the inverted tube test, which decreased to a few seconds (< 10 s, see video) when sprayed on a surface thermostated to 35 °C. This time was considered appropriate for nasal administration (10–57 s to 5 min) to permit easy administration as a sol and rapid gelation for retaining the formulation at the site of application, avoiding drainage from the nasal cavity and overcoming mucociliary clearance (approximately 15–20 min) [40,44,51,54]. As a hydrogel, G1 could absorb a small amount of water due to the presence of water in the solution/hydrogel. This water uptake capacity determines in vivo the rapid absorption of water from nasal mucus and, consequently, the interpenetration of the chitosan chain with mucin, which favors mucoadhesion [41,51,54,55]. Dehydration of the nasal mucosa can be avoided due to the low water absorption of this thermosensitive hydrogel. The detachment force confirmed that G1 showed good in vitro mucoadhesion properties. In the literature, mucoadhesion strength values in the range of 22–30 g/cm^2 are satisfactory for increasing nasal residence time without damage or irritation of the mucosa [54–56].

In the hydrogel, DMF was homogeneously dispersed, as demonstrated by DSC, and was released from G1, which linearly permeated the hydrophilic membrane from 15 min to 120 min. From this result, it can be assumed that the DMF released from G1 can diffuse through the hydrophilic mucus and then, as demonstrated in our previous works, permeate the nasal epithelium, reaching the blood and/or the brain, due to the enhanced penetration of CH and cyclodextrin [20,22–24,26].

The strengths, challenges and opportunities within the market of this research are highlighted in the SWOT analysis reported in Table S2.

5. Conclusions

This research showed that a thermosensitive chitosan/glycerophosphate hydrogel could be a helpful formulation for DMF nasal administration. Complexing DMF with HP-β-CD significantly improved its water solubility, allowing for a higher drug concentration in the formulation. The preparation method of the hydrogel precursor solution is pivotal for effective DMF loading. The study highlights that the acidic environment required for CH solubilization can lead to hydrolytic degradation of DMF; in fact, only G1 S is optimal for DMF loading (drug content of 92 %) and provides stability to DMF for 21 days. All the tests show that G1 S meets all necessary nasal liquid dosage requirements, including pH, osmolality, viscosity, and droplet size distribution. In particular, the viscosity of G1 S is such that its nasal administration using a nasal spray device. After administration, the short gelation time will ensure a prolonged residence time in the nasal cavity, counteracting mucociliary clearance. In addition, osmolality, mucoadhesiveness and the presence of penetration enhancers such as CH and HP-β-CD will be able to promote the permeation of DMF released from the hydrogel across the nasal mucosa. Therefore, these results provide a good starting point for exploring the potential use of the intranasal route as an alternative approach to oral DMF administration in treating multiple sclerosis with DMF to reduce side effects and increase adherence to therapy and bioavailability in the brain. Given the epidemiologic data and economic burden of MS, the future societal impact of this research may be high as it is an attempt at a possible effective management strategy to improve patient outcomes.

Supplementary data to this article can be found online at https://doi.org/10.1016/j.ijbiomac.2024.134908.

Funding

This research was partially funded by Fondo di Finanziamento per le Attività Base di Ricerca FFABR 2017 (granted to G. Rassu) and by the Foundation1 of Sardinia (Bando Fondazione di Sardegna – 2018-2020 e 2021 – Progetti di ricerca di base dipartimentali"; grant number J89J21015120005) (granted to E. Gavini).

Artwork

The graphical abstract and Fig. 1 were created with BioRender.com.

CRediT authorship contribution statement

Noelia Nieto González: Writing – original draft, Visualization, Investigation, Formal analysis, Data curation. **Giovanna Rassu:** Writing – review & editing, Visualization, Validation, Supervision, Project administration, Funding acquisition, Conceptualization. **Massimo Cossu:** Investigation, Formal analysis. **Laura Catenacci:** Writing – original draft, Visualization, Formal analysis, Data curation. **Milena L. Sorrenti:** Writing – review & editing, Resources, Data curation, Conceptualization. **Eleonora Sofia Cama:** Writing – original draft, Investigation, Formal analysis. **Carla Serri:** Visualization, Resources. **Paolo Giunchedi:** Writing – review & editing, Validation, Supervision, Resources. **Elisabetta Gavini:** Writing – review & editing, Validation, Supervision, Funding acquisition, Conceptualization.

Declaration of competing interest

The authors declare that they have no known competing financial interests or personal relationships that could have appeared to influence the work reported in this paper. Giovanna Rassu reports financial support was provided by Fondo di Finanziamento per le Attività Base di Ricerca FFABR 2017. Gavini Elisabetta reports financial support was provided by Foundation of Sardinia. If there are other authors, they declare that they have no known competing financial interests or personal relationships that could have appeared to influence the work reported in this paper.

Data availability

The datasets generated and/or analyzed during the current study are available from the corresponding author upon reasonable request.

Acknowledgements

Noelia Nieto González gratefully acknowledges the University of Sassari for the financial support of her PhD scholarship.

References

[1] R. Dobson, G. Giovannoni, Multiple sclerosis – a review, Eur. J. Neurol. 26 (2019) 27–40, https://doi.org/10.1111/ene.13819.
[2] AISM, n.d. Barometro Della Sclerosi Multipla 2022.
[3] D.S. Goodin, The epidemiology of multiple sclerosis, in: Handbook of Clinical Neurology, Elsevier, 2014, pp. 231–266, https://doi.org/10.1016/B978-0-444-52001-2.00010-8.
[4] A. Compston, A. Coles, Multiple sclerosis, Lancet 372 (2008) 1502–1517, https://doi.org/10.1016/S0140-6736(08)61620-7.
[5] C.A. Dendrou, L. Fugger, M.A. Friese, Immunopathology of multiple sclerosis, Nat. Rev. Immunol. 15 (2015) 545–558, https://doi.org/10.1038/nri3871.
[6] T. Derfuss, M. Mehling, A. Papadopoulou, A. Bar-Or, J.A. Cohen, L. Kappos, Advances in oral immunomodulating therapies in relapsing multiple sclerosis, Lancet Neurol. 19 (2020) 336–347, https://doi.org/10.1016/S1474-4422(19)30391-6.

[7] E.D. Deeks, Dimethyl fumarate: a review in relapsing-remitting MS, Drugs 76 (2016) 243–254, https://doi.org/10.1007/s40265-015-0528-1.
[8] S.K. Yadav, D. Soin, K. Ito, S. Dhib-Jalbut, Insight into the mechanism of action of dimethyl fumarate in multiple sclerosis, J. Mol. Med. 97 (2019) 463–472, https://doi.org/10.1007/s00109-019-01761-5.
[9] R. Gold, D.L. Arnold, A. Bar-Or, R.J. Fox, L. Kappos, O. Mokliatchouk, X. Jiang, J. Lyons, S. Kapadia, C. Miller, Long-term safety and efficacy of dimethyl fumarate for up to 13 years in patients with relapsing-remitting multiple sclerosis: final ENDORSE study results, Mult. Scler. J. 28 (2022) 801–816, https://doi.org/10.1177/13524585211037909.
[10] R. Alroughani, R. Das, N. Penner, J. Pultz, C. Taylor, S. Eraly, Safety and efficacy of delayed-release dimethyl fumarate in pediatric patients with relapsing multiple sclerosis (FOCUS), Pediatr. Neurol. 83 (2018) 19–24, https://doi.org/10.1016/j.pediatrneurol.2018.03.007.
[11] R. Alroughani, P. Huppke, M. Mazurkiewicz-Beldzinska, A. Blaschek, M. Valis, G. Aaen, J. Pultz, X. Peng, V. Beynon, Delayed-release dimethyl fumarate safety and efficacy in pediatric patients with relapsing-remitting multiple sclerosis, Front. Neurol. 11 (2021) 606418, https://doi.org/10.3389/fneur.2020.606418.
[12] B. Narapureddy, D. Dubey, Clinical evaluation of dimethyl fumarate for the treatment of relapsing-remitting multiple sclerosis: efficacy, safety, patient experience and adherence, Patient Prefer. Adherence 13 (2019) 1655–1666, https://doi.org/10.2147/PPA.S187529.
[13] EMA, Assessment Report - Tecfidera EMA/800904/2013 Corr. 1, 2013.
[14] M. Agrawal, Shailendra Saraf, Swarnlata Saraf, S.K. Dubey, A. Puri, U. Gupta, P. Kesharwani, V. Ravichandiran, P. Kumar, V.G.M. Naidu, U.S. Murty, Alexander Ajazuddin, Stimuli-responsive In situ gelling system for nose-to-brain drug delivery, J. Control. Release 327 (2020) 235–265, https://doi.org/10.1016/j.jconrel.2020.07.044.
[15] S. Duchi, H. Ovadia, E. Touitou, Nasal administration of drugs as a new non-invasive strategy for efficient treatment of multiple sclerosis, J. Neuroimmunol. 258 (2013) 32–40, https://doi.org/10.1016/j.jneuroim.2013.02.013.
[16] A. Salis, G. Rassu, M. Budai-Szűcs, I. Benzoni, E. Csányi, S. Berkó, M. Maestri, P. Dionigi, E.P. Porcu, E. Gavini, P. Giunchedi, Development of thermosensitive chitosan/glicerophospate injectable *in situ* gelling solutions for potential application in intraoperative fluorescence imaging and local therapy of hepatocellular carcinoma: a preliminary study, Expert Opin. Drug Deliv. 12 (2015) 1583–1596, https://doi.org/10.1517/17425247.2015.1042452.
[17] C. Coisne, S. Tilloy, E. Monflier, D. Wils, L. Fenart, F. Gosselet, Cyclodextrins as emerging therapeutic tools in the treatment of cholesterol-associated vascular and neurodegenerative diseases, Molecules 21 (2016) 1748, https://doi.org/10.3390/molecules21121748.
[18] G. Rassu, S. Fancello, M. Roldo, M. Malanga, L. Szente, R. Migheli, E. Gavini, P. Giunchedi, Investigation of cytotoxicity and cell uptake of cationic beta-cyclodextrins as valid tools in nasal delivery, Pharmaceutics 12 (2020) 658, https://doi.org/10.3390/pharmaceutics12070658.
[19] G. Rassu, M. Sorrenti, L. Catenacci, B. Pavan, L. Ferraro, E. Gavini, M.C. Bonferoni, P. Giunchedi, A. Dalpiaz, Versatile nasal application of cyclodextrins: excipients and/or actives? Pharmaceutics 13 (2021) 1180, https://doi.org/10.3390/pharmaceutics13081180.
[20] A. Yalcin, E. Soddu, E. Turunc Bayrakdar, Y. Uyanikgil, L. Kanit, G. Armagan, G. Rassu, E. Gavini, P. Giunchedi, Neuroprotective effects of engineered polymeric nasal microspheres containing hydroxypropyl-β-cyclodextrin on β-amyloid (1-42)–induced toxicity, J. Pharm. Sci. 105 (2016) 2372–2380, https://doi.org/10.1016/j.xphs.2016.05.017.
[21] E. Elmowafy, M.E. Soliman, Polysaccharide-based platforms for nasal delivery: design, features, and perspectives, J. Pharm. Investig. (2023), https://doi.org/10.1007/s40005-023-00626-x.
[22] E. Gavini, G. Rassu, L. Ferraro, S. Beggiato, A. Alhalaweh, S. Velaga, N. Marchetti, P. Bandiera, P. Giunchedi, A. Dalpiaz, Influence of polymeric microcarriers on the in vivo intranasal uptake of an anti-migraine drug for brain targeting, Eur. J. Pharm. Biopharm. 83 (2013) 174–183, https://doi.org/10.1016/j.ejpb.2012.10.010.
[23] E. Gavini, G. Rassu, L. Ferraro, A. Generosi, J.V. Rau, A. Brunetti, P. Giunchedi, A. Dalpiaz, Influence of chitosan glutamate on the in vivo intranasal absorption of Rokitamycin from microspheres, J. Pharm. Sci. 100 (2011) 1488–1502, https://doi.org/10.1002/jps.22382.
[24] G. Rassu, L. Ferraro, B. Pavan, P. Giunchedi, E. Gavini, A. Dalpiaz, The role of combined penetration enhancers in nasal microspheres on in vivo drug bioavailability, Pharmaceutics 10 (2018) 206, https://doi.org/10.3390/pharmaceutics10040206.
[25] G. Rassu, E. Gavini, H. Jonassen, Y. Zambito, S. Fogli, M.C. Breschi, P. Giunchedi, New chitosan derivatives for the preparation of rokitamycin loaded microspheres designed for ocular or nasal administration, J. Pharm. Sci. 98 (2009) 4852–4865, https://doi.org/10.1002/jps.21751.
[26] G. Rassu, E. Soddu, M. Cossu, A. Brundu, G. Cerri, N. Marchetti, L. Ferraro, R. F. Regan, P. Giunchedi, E. Gavini, A. Dalpiaz, Solid microparticles based on chitosan or methyl-β-cyclodextrin: a first formulative approach to increase the nose-to-brain transport of deferoxamine mesylate, J. Control. Release 201 (2015) 68–77, https://doi.org/10.1016/j.jconrel.2015.01.025.
[27] G. Rassu, E. Soddu, M. Cossu, E. Gavini, P. Giunchedi, A. Dalpiaz, Particulate formulations based on chitosan for nose-to-brain delivery of drugs. A review, J. Drug Deliv. Sci. Technol. 32 (2016) 77–87, https://doi.org/10.1016/j.jddst.2015.05.002.
[28] P. Rahmanian-Devin, V. Baradaran Rahimi, V.R. Askari, Thermosensitive chitosan-β-Glycerophosphate hydrogels as targeted drug delivery systems: an overview on preparation and their applications, Adv. Pharmacol. Pharm. Sci. 2021 (2021) 1–17, https://doi.org/10.1155/2021/6640893.
[29] T. Higuchi, A phase solubility technique, Adv. Anal. Chem. Instrum. 4 (1965) 117–211.
[30] E. Esposito, R. Cortesi, M. Drechsler, J. Fan, B.M. Fu, L. Calderan, S. Mannucci, F. Boschi, C. Nastruzzi, Nanoformulations for dimethyl fumarate: physicochemical characterization and in vitro/in vivo behavior, Eur. J. Pharm. Biopharm. 115 (2017) 285–296, https://doi.org/10.1016/j.ejpb.2017.04.011.
[31] R. Ahmadi, J.D. de Bruijn, Biocompatibility and gelation of chitosan–glycerol phosphate hydrogels, J. Biomed. Mater. Res. A 86A (2008) 824–832, https://doi.org/10.1002/jbm.a.31676.
[32] T. Masiuk, P. Kadakia, Z. Wang, Development of a physiologically relevant dripping analytical method using simulated nasal mucus for nasal spray formulation analysis, J. Pharm. Anal. 6 (2016) 283–291, https://doi.org/10.1016/j.jpha.2016.05.003.
[33] C. Juliano, M. Cossu, P. Pigozzi, G. Rassu, P. Giunchedi, Preparation, in vitro characterization and preliminary in vivo evaluation of buccal polymeric films containing chlorhexidine, AAPS PharmSciTech 9 (2008) 1153–1158, https://doi.org/10.1208/s12249-008-9153-6.
[34] E. Gavini, A. Hegge, G. Rassu, V. Sanna, C. Testa, G. Pirisino, J. Karlsen, P. Giunchedi, Nasal administration of carbamazepine using chitosan microspheres: in vitro/in vivo studies, Int. J. Pharm. 307 (2006) 9–15, https://doi.org/10.1016/j.ijpharm.2005.09.013.
[35] J.D. Ehrick, S.A. Shah, C. Shaw, V.S. Kulkarni, I. Coowanitwong, S. De, J.D. Suman, Considerations for the development of nasal dosage forms, in: P. Kolhe, M. Shah, N. Rathore (Eds.), Sterile Product Development, AAPS Advances in the Pharmaceutical Sciences Series, Springer New York, New York, NY, 2013, pp. 99–144, https://doi.org/10.1007/978-1-4614-7978-9_5.
[36] G. Rassu, A. Salis, E.P. Porcu, P. Giunchedi, M. Roldo, E. Gavini, Composite chitosan/alginate hydrogel for controlled release of deferoxamine: a system to potentially treat iron dysregulation diseases, Carbohydr. Polym. 136 (2016) 1338–1347, https://doi.org/10.1016/j.carbpol.2015.10.048.
[37] D. Marx, G. Williams, M. Birkhoff, Intranasal drug administration — an attractive delivery route for some drugs, in: O. Vallisuta, S. Olimat (Eds.), Drug Discovery and Development - From Molecules to Medicine, InTech, 2015, https://doi.org/10.5772/59468.
[38] E.S. Cama, L. Catenacci, S. Perteghella, M. Sorrenti, M.R. Caira, G. Rassu, E. Gavini, P. Giunchedi, M.C. Bonferoni, Design and development of a chitosan-based nasal powder of dimethyl fumarate-cyclodextrin binary systems aimed at nose-to-brain administration. A stability study, Int. J. Pharm. 659 (2024) 124216, https://doi.org/10.1016/j.ijpharm.2024.124216.
[39] Y. Yu, Y. Cheng, J. Tong, L. Zhang, Y. Wei, M. Tian, Recent advances in thermo-sensitive hydrogels for drug delivery, J. Mater. Chem. B 9 (2021) 2979–2992, https://doi.org/10.1039/D0TB02877K.
[40] M. Wang, X. Ma, S. Zong, Y. Su, R. Su, H. Zhang, Y. Liu, C. Wang, Y. Li, The prescription design and key properties of nasal gel for CNS drug delivery: a review, Eur. J. Pharm. Sci. 192 (2024) 106623, https://doi.org/10.1016/j.ejps.2023.106623.
[41] Q. Wang, Z. Zuo, C.K.C. Cheung, S.S.Y. Leung, Updates on thermosensitive hydrogel for nasal, ocular and cutaneous delivery, Int. J. Pharm. 559 (2019) 86–101, https://doi.org/10.1016/j.ijpharm.2019.01.030.
[42] M. Agrawal, Swarnlata Saraf, Shailendra Saraf, S.G. Antimisiaris, M.B. Chougule, S. A. Shoyele, A. Alexander, Nose-to-brain drug delivery: an update on clinical challenges and progress towards approval of anti-Alzheimer drugs, J. Control. Release 281 (2018) 139–177, https://doi.org/10.1016/j.jconrel.2018.05.011.
[43] A. Chenite, Rheological characterisation of thermogelling chitosan/glycerol-phosphate solutions, Carbohydr. Polym. 46 (2001) 39–47, https://doi.org/10.1016/S0144-8617(00)00281-2.
[44] H. Gholizadeh, E. Messerotti, M. Pozzoli, S. Cheng, D. Traini, P. Young, A. Kourmatzis, C. Caramella, H.X. Ong, Application of a thermosensitive in situ gel of chitosan-based nasal spray loaded with tranexamic acid for localised treatment of nasal wounds, AAPS PharmSciTech 20 (2019) 299, https://doi.org/10.1208/s12249-019-1517-6.
[45] M. Gao, X. Shen, S. Mao, Factors influencing drug deposition in thenasal cavity upon delivery via nasal sprays, J. Pharm. Investig. 50 (2020) 251–259, https://doi.org/10.1007/s40005-020-00482-z.
[46] A. Popielec, T. Loftsson, Effects of cyclodextrins on the chemical stability of drugs, Int. J. Pharm. 531 (2017) 532–542, https://doi.org/10.1016/j.ijpharm.2017.06.009.
[47] A.A. Habib, S.F. Hammad, M.M. Amer, A.H. Kamal, Stability indicating RP-HPLC method for determination of dimethyl fumarate in presence of its main degradation products: application to degradation kinetics, J. Sep. Sci. 44 (2021) 726–734, https://doi.org/10.1002/jssc.202001007.
[48] C.P. Costa, S. Barreiro, J.N. Moreira, R. Silva, H. Almeida, J.M. Sousa Lobo, A. C. Silva, In vitro studies on nasal formulations of nanostructured lipid carriers (NLC) and solid lipid nanoparticles (SLN), Pharmaceuticals 14 (2021) 711, https://doi.org/10.3390/ph14080711.
[49] S. Jagdale, N. Shewale, B.S. Kuchekar, Optimization of Thermoreversible *in situ* nasal gel of Timolol maleate, Scientifica 2016 (2016) 1–11, https://doi.org/10.1155/2016/6401267.
[50] R. Scherließ, Nasal formulations for drug administration and characterization of nasal preparations in drug delivery, Ther. Deliv. 11 (2020) 183–191, https://doi.org/10.4155/tde-2019-0086.
[51] R.R. Verekar, S.S. Gurav, U. Bolmal, Thermosensitive mucoadhesive in situ gel for intranasal delivery of Almotriptan malate: formulation, characterization, and

evaluation, J. Drug Deliv. Sci. Technol. 58 (2020) 101778, https://doi.org/10.1016/j.jddst.2020.101778.
[52] S. Jauhari, A.K. Dash, A mucoadhesive in situ gel delivery system for paclitaxel, AAPS PharmSciTech 7 (2006) E154–E159, https://doi.org/10.1208/pt070253.
[53] M. Kumar, P. Upadhayay, R. Shankar, M. Joshi, S. Bhatt, A. Malik, Chlorpheniramine maleate containing chitosan-based nanoparticle-loaded thermosensitive in situ gel for management in allergic rhinitis, Drug Deliv. Transl. Res. 9 (2019) 1017–1026, https://doi.org/10.1007/s13346-019-00639-w.
[54] P. Mura, N. Mennini, C. Nativi, B. Richichi, In situ mucoadhesive-thermosensitive liposomal gel as a novel vehicle for nasal extended delivery of opiorphin, Eur. J. Pharm. Biopharm. 122 (2018) 54–61, https://doi.org/10.1016/j.ejpb.2017.10.008.
[55] B. Menchicchi, J.P. Fuenzalida, K.B. Bobbili, A. Hensel, M.J. Swamy, F. M. Goycoolea, Structure of chitosan determines its interactions with mucin, Biomacromolecules 15 (2014) 3550–3558, https://doi.org/10.1021/bm5007954.
[56] T. Adnet, A.-C. Groo, C. Picard, A. Davis, S. Corvaisier, M. Since, F. Bounoure, C. Rochais, L. Le Pluart, P. Dallemagne, A. Malzert-Fréon, Pharmacotechnical development of a nasal drug delivery composite nanosystem intended for Alzheimer's disease treatment, Pharmaceutics 12 (2020) 251, https://doi.org/10.3390/pharmaceutics12030251.